

## Efficient regime of the plasma wakefield accelerator

K. V. Lotov

*Budker Institute of Nuclear Physics, Lavrent'ev Ave. 11, 630090, Novosibirsk, Russia*

Plasmas can sustain very large electric fields that are many orders of magnitude higher than those in conventional accelerating structures. This property is used in plasma wakefield accelerators (PWFA), in which one electron beam drives the high amplitude field in the plasma, and another beam (witness) is accelerated by this field. Reviews of PWFA basics can be found in [1, 2].

To compete with conventional accelerators, PWFA must have high efficiency  $\eta$ , low energy spread of the accelerated beam, and high transformer ratio  $R$  (i.e., the ratio of longitudinal electric fields in two beams). The energy spread can be minimized by matching the witness shape and the plasma wave. As to the efficiency and transformer ratio, there is an unpleasant choice between them, since high accelerating fields require a large fraction of plasma energy to be left behind the witness. This choice is relieved for the efficient blowout regime that is described further. In this regime, all plasma electrons are ejected off the beam propagation channel, and an electron-free region (the cavern) is formed around the drive beam.

As the measure of beam-plasma energy exchange, we use the energy flux in the co-moving window [3]. For axisymmetric beams and cylindrical coordinates  $(r, \varphi, z)$ , it reads as

$$\Psi = \int_0^{\infty} \left( \frac{c}{8\pi} \left( (E_r - B_\varphi)^2 + E_z^2 \right) + \sum_{\text{u.v.}} (\gamma - 1) mc^2 (c - v_z) \right) 2\pi r dr, \quad (1)$$

where the summation is carried out over plasma electrons in the unit volume,  $\gamma$  is the relativistic factor of plasma electrons,  $v_z$  is their longitudinal velocity, and other notation is common. The variation of  $\Psi$  with the co-moving coordinate  $\xi = z - ct$  shows the work of different beam slices against the wakefield:

$$\frac{\partial \Psi}{\partial \xi} = \int_0^{\infty} j_{bz} E_z 2\pi r dr, \quad (2)$$

where  $j_{bz} = -en_b c$  is the beam current density. In what follows, we use the dimensionless quantities and denote them by tildes, for example,

$$\tilde{\xi} = \frac{\xi \omega_p}{c}, \quad \tilde{n} = \frac{n}{n_0}, \quad \tilde{\Psi} = \frac{4\pi e^2 \Psi}{m^2 c^5}, \quad \omega_p = \sqrt{\frac{4\pi n_0 e^2}{m}}, \quad (3)$$

$$\tilde{I}_b = \frac{e I_b}{m c^3}, \quad \tilde{E}_z = \frac{E_z}{\sqrt{4\pi n_0 m c^2}}, \quad \tilde{N}_d = \frac{N_d}{N_0} \equiv \frac{N_d}{n_0} \left( \frac{\omega_p}{c} \right)^3, \quad (4)$$

where  $n$  and  $n_0$  are densities of plasma electrons and ions,  $I_b$  is the beam current,  $N_d$  is the number of particles in the driver. All simulations presented in the paper are made with the two-dimensional axisymmetric hybrid code LCODE [4, 5].

The efficient acceleration is realized when the driver operates in the “strong beam” blowout regime [3], the most part of the driver and the whole witness are inside the cavern, and the beams are shaped to flatten the profile of  $E_z$ .

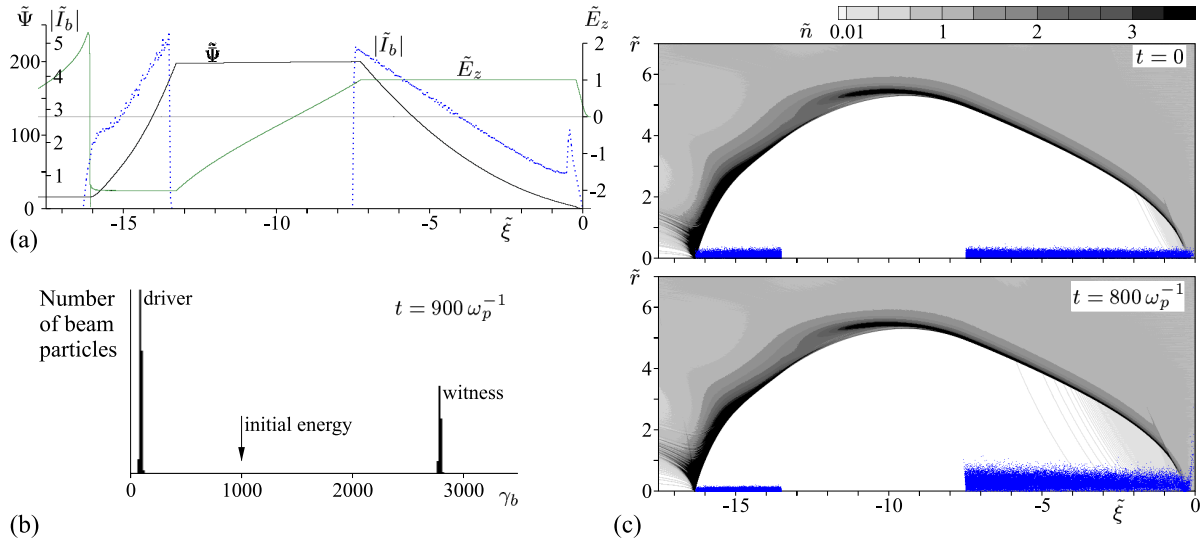


Figure 1: (a) Dependence of the beam current ( $\tilde{I}_b$ ), on-axis electric field ( $\tilde{E}_z$ ), and energy flux ( $\tilde{\Psi}$ ) on  $\tilde{\xi}$  at the beginning of beam-plasma interaction; (b) the resultant energy spectrum of two beams; (c) beam portraits (dots) plotted on the maps of plasma electron density at the beginning of interaction (upper picture) and shortly before the driver depletion (lower picture).

An example of beam and plasma dynamics in the efficient regime is shown in Fig. 1. Here both beams initially have the radius  $\sigma_r = 0.1 c/\omega_p$ , emittance  $10^{-4} c/\omega_p$  rad, and the relativistic factor  $\gamma_b = 1000$ . In simulations we use  $7.5 \cdot 10^6$  macroparticles for the beams and  $2 \cdot 10^4$  macroparticles for the plasma. The time step is  $5 \omega_p^{-1}$ , the grid size on  $(\tilde{r}, \tilde{\xi})$  plane is 0.005, with automatic decrease of the  $\tilde{\xi}$ -step down to  $5 \cdot 10^{-6}$  near the end of the cavern. The initial profile of the beam current is numerically adjusted to have  $\tilde{E}_z = 1$  inside the driver and  $\tilde{E}_z = -2$  inside the witness. The required shape of the driver is close to the triangular one (Fig. 1a), just as it is for the linearly responding plasma [6]. In the run presented, 80% of the initial driver energy is transferred to the witness (Fig. 1b), about 10% of the energy remains with the driver, and 10% is left in the plasma. The final energy spread of the witness is 0.35%, and this number is determined mainly by the accuracy of the witness shape control.

The constituents of the efficient regime are the following. The high-current (“strong”)

driver makes the wide cavern and provides a high energy content of the wakefield. Since the driver is not very short, this energy is stored mostly in the electromagnetic field [3] and can be easily withdrawn from the plasma. Operating in the blowout regime allows us to leave a relatively small portion of the energy behind the witness even for high accelerating rates. The blowout regime also ensures invariance of the wakefield during the acceleration cycle (Fig. 1c) and uniformity of the longitudinal field across the beams. With the beam shaping, we obtain a small energy spread of the witness and efficient utilization of the driver energy.

The number of particles in the witness in Fig. 1 is  $N_w \approx 90 N_0$ , in the driver it is twice higher. For the plasma density  $n_0 = 10^{15} \text{cm}^{-3}$ , this is a huge number:  $N_w \approx 4 \cdot 10^{11}$  particles. For higher plasma densities,  $N_w$  and  $N_d$  are correspondingly lower since  $N_0 \propto n_0^{-1/2}$ . Thus, we can formulate three necessary conditions for operation in the extremely efficient regime. First, a longitudinal beam compression is required to prepare a high-current driver. Second, a relatively high plasma density is needed to access the efficient regime with conceivable beam charges. Third, a fine control of driver and witness shapes is required. All three conditions can be fulfilled, to some extent, in next-generation PWFA facilities that are currently developed in Stanford and in Novosibirsk. With the drive beam from the VEPP-5 injection complex, it will be possible to accelerate up to  $3 \cdot 10^9$  particles with 30% driver-to-witness efficiency, 70% plasma-to-witness efficiency, and energy spread lower than 10% [7].

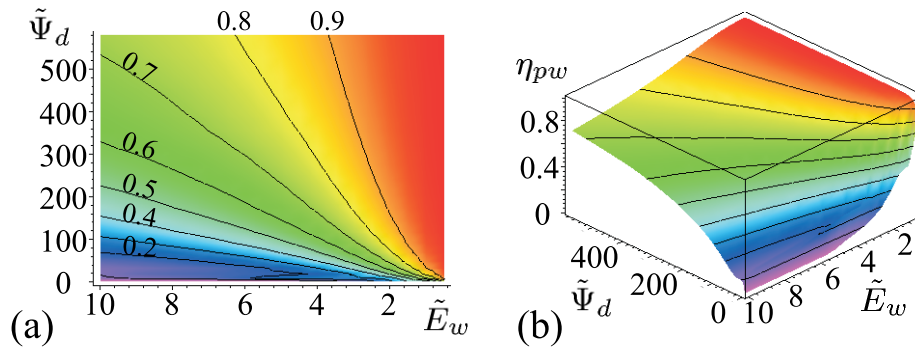


Figure 2: The plasma-to-witness efficiency  $\eta_{pw}$  as a function of the energy flux behind the driver  $\tilde{\Psi}_d$  and accelerating field  $\tilde{E}_w$ : (a) map of level curves and (b) surface plot.

Simulations of various driver shapes have shown that the ability of the wakefield to accelerate particles is mainly determined by the energy flux  $\tilde{\Psi}_d$  behind the driver and weakly depend on the particular driver shape. Therefore, we can plot the universal map of maximum plasma-to-witness efficiency  $\eta_{pw}$  on the  $(\tilde{E}_w, \tilde{\Psi}_d)$  plane (Fig. 2). The efficiency is calculated as  $\eta_{pw} = 1 - \tilde{\Psi}_w / \tilde{\Psi}_d$ , where  $\tilde{\Psi}_w$  is the energy flux behind the witness. It is seen that at high energy

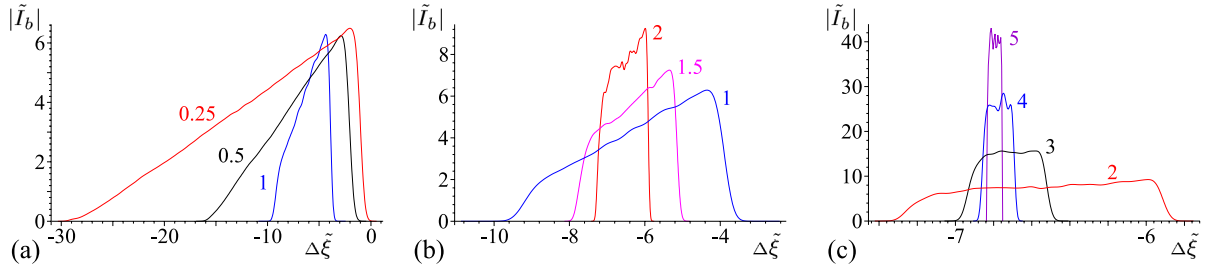


Figure 3: The optimum witness shape for various accelerating fields  $\tilde{E}_w$  (marked near the graphs). The displacement  $\Delta\tilde{\xi}$  is measured from the point of zero  $\tilde{E}_z$ .

fluxes the efficiency is high even for high accelerating fields.

The required shape of the witness depends on the accelerating field. For a low field ( $\tilde{E}_w \ll 1$ ), the witness must have a linearly decreasing current to have a small energy spread (Fig. 3a). For high fields ( $\tilde{E}_w \gg 1$ ), the required current profile is close to the rectangular one (Fig. 3c). The transition between the limiting cases is shown in Fig. 3b. The graphs in Fig. 3 are made for  $\tilde{\Psi}_d = 580$ . For lower energy fluxes, the dependence of the witness shape on  $\tilde{E}_w$  remains qualitatively the same.

This work was supported by Science Support Foundation, SB RAS Lavrent'ev Grant for young researchers, Russian Foundation for Basic Research (grant 03-02-16160a), and Russian Ministry of Science (grant NSh-229.2003.2).

## References

- [1] E. Esarey, P. Sprangle, J. Krall, and A. Ting, *IEEE Trans. Plasma Sci.* **24**, 252 (1996).
- [2] C. Joshi, et al., *Phys. Plasmas* **9**, 1845 (2002).
- [3] K. V. Lotov, *Phys. Rev. E* **69**, 046405 (2004).
- [4] K. V. Lotov, *Phys. Rev. ST Accel. Beams* **6**, 061301 (2003).
- [5] K. V. Lotov, *Phys. Plasmas* **5**, 785 (1998).
- [6] T. Katsouleas, *Phys. Rev. A.* **33**, 2056 (1986).
- [7] A.V.Burdakov, A.M.Kudryavtsev, P.V.Logatchov, K.V.Lotov, A.V.Petrenko, and A.N.Skrinsky, *Experimental Plasma Wakefield Acceleration Project at the VEPP-5 Injection Complex*, this Proceedings.